**In Search of the Chemical Basis of the Hemolytic Potential of Silicas**

UNIVERSITÀ DEGLI STUDI DI TORINO

# In Search of the Chemical Basis of the Hemolytic Potential of Silicas

*Cristina Pavan,*[§,†] *Maura Tomatis,*[§,†,‡] *Mara Ghiazza,*[§,†,‡] *Virginie Rabolli,*[‖] *Vera Bolis,*[†,‡] *Dominique Lison,*[‖] *and Bice Fubini**[§,†,‡]

[§]"G. Scansetti" Interdepartmental Center for Studies on Asbestos and Other Toxic Particulates, Department of Chemistry, University of Torino, Via P. Giuria 7, 10125 Turin, Italy

[†]Department of Chemistry, University of Torino, Via P. Giuria 7, 10125 Turin, Italy

[‡]Interdepartmental Center for Nanostructured Interfaces and Surfaces, Department of Chemistry, University of Torino, Via P. Giuria 7, 10125 Turin, Italy

[‖]Louvain Center for Toxicology and Applied Pharmacology (LTAP), Université Catholique de Louvain, Avenue E. Mounier, B1.52.12, 1200 Brussels, Belgium

KEYWORDS. Red blood cells, membranolysis, silica, quartz, surface silanols.

TABLE OF CONTENT

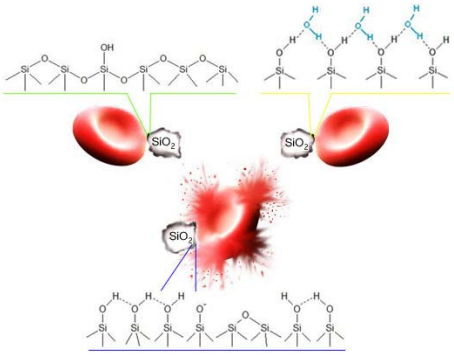

ABSTRACT. The membranolytic activity of silica particles toward red blood cells (RBCs) has been known for a long time and sometimes associated to silica pathogenicity. However, the molecular mechanism and the reasons why hemolysis differs according to the silica form are still obscure. A panel of 15 crystalline (pure and commercial) and amorphous (pyrogenic, precipitated from aqueous solutions, vitreous) silica samples differing in size, origin, morphology and surface chemical composition were selected and specifically prepared. Silica particles were grouped into six groups to compare their potential in disrupting RBC membranes, so that one single property differed in each group, while other features were constant. Free radical production and crystallinity were not strict determinants of the hemolytic activity. Particle curvature and morphology modulated the hemolytic effect, but silanols and siloxane bridges at the surface were the main actors. Hemolysis was unrelated to the overall concentration of silanols as fully rehydrated surfaces (such as those obtained from aqueous solution) were inert and one pyrogenic silica also lost its membranolytic potential upon progressive dehydration. Overall results are consistent with a model whereby hemolysis is determined by a defined surface distribution of dissociated/undissociated silanols and siloxane groups strongly interacting with specific epitopes on the RBC membrane.

## INTRODUCTION

Silica is one of the most studied material because of its extremely wide field of industrial applications. It is also extensively investigated by toxicologists because of its pathogenicity, which may lead to the development of silicosis, lung cancer and autoimmune diseases in humans exposed to respirable crystalline silica dusts.[1-3] However, biological responses to crystalline silica dusts are extremely variable, and it is generally agreed that quartz (the most common crystalline polymorph) is a "variable entity" as far as its pathogenic activity is concerned.[4,5] Differences in surface characteristics of crystalline dusts – mostly obtained by mechanical fragmentation – are suggested to be the main source of this variability.[6]

So far, amorphous silicas have been considered non harmful, and have been widely employed even in the food and drug industry without any apparent health concern. With the advent of nanotechnology and the use of – generally amorphous – silica nanoparticles (NPs) in several applications, including biomedicine, their potential toxicity has been largely studied. A great variability has also been found among the biological responses recorded with a variety of silica NPs, the source of which being generally assigned to variable size and preparation routes.[7]

Thus the molecular mechanisms underlying biological responses to silica particles are still a puzzle,[5] the main reasons being the diversity of existing silica samples and the complexity of interactions with biomolecules.[8]

The hemolytic potential of silica particles has long been known.[9] Even if red blood cells (RBCs) play no part in the pathogenesis of silicosis or cancer, the hemolytic activity of silica particles has been traditionally considered somehow predictive of their pathogenicity. It is an easy, sensitive and rapid endpoint to investigate the membranolytic activity of particulates. Indeed the RBC membrane is likely to represent a simple model of biological membranes, which are important targets of silica toxicity.[10] Recently, with the rising interest in

nanostructured silica materials for biomedical applications, the assessment of their hemolytic potential is back in vogue to evaluate toxic effects when intravenously administered as a drug carrier,[11] or as a marker of pathogenicity associated to adverse biological responses.[12-16]

The potential of silica particles to generate reactive oxygen species (ROS) has been suggested to be the cause of their hemolytic activity.[17,18] In particular, Zhang and co-workers (2012)[18] suggested a hydroxyl radical-based mechanism for one fumed silica. Other studies, however, showed no correlation between particle-derived ROS and silica-induced hemolysis.[13,19,20]

The degree of hydrophilicity (related to surface silanols -SiOH) and hydrophobicity (related to surface siloxanes -Si-O-Si-) of silica particles is another proposed determinant of toxicity.[21-24] Thermal treatment of silica dusts stabilizes the structure, reduces the population of surface silanols,[25] and leads to a reduction of their hemolytic activity.[26] In contrast, hydrothermal treatment causes an increment in silanol population.[27] Pandurangi et al. (1990)[26] reported a correlation between the concentration of free surface -SiOH groups and the hemolytic activity, while Murashov and co-workers (2006)[28] claimed the density of the geminal silanol groups (two -OH groups linked to the same silicon atom) to be responsible for hemolysis. Other chemical treatments severely affecting the surface and consequently depressing the hemolytic activity have been ascribed to the involvement of silanols: adsorption of polymers (e.g. poly(2-vinylpyridine-N-oxide) – PVPNO),[10,29] proteins and lipids (e.g. albumin, lecithin, serum, plasma corona),[29-31] chloroquine,[32,33] and aluminum compounds (e.g. $AlCl_3$, aluminosilicate compounds, aluminium lactate).[10,16,34] A decrease in hemolytic activity was also observed by replacing the hydroxyl groups with trimethylsilyl groups[35] and by etching silica particles with hydrofluoric acid.[36,37] Recent studies on the porous structure of amorphous silica NPs revealed that mesoporosity for particles of similar size reduced their hemolytic activity because of the depletion of surface silanol groups

accessible to the RBC membranes.[38-40] In addition, particle size appears related to hemolytic activity for both micro and nano-silicas. Considering micrometric-sized particles, the smaller quartz particles were found more membranolytic than the larger ones.[36,41] In contrast, hemolytic activity increased with increasing particle size with fumed silica,[42] mesoporous silica,[11] and colloidal amorphous silica NPs.[33] Thomassen et al. (2011)[43] found that an increase in size (in terms of curvature) for low density fractal aggregates determines a decrease in hemolysis because the number of primary particles in the outer shell per unit area decreased; in the case of dense aggregates hemolytic activity increased with larger sizes, behaving as primary particles. Finally, the hemolytic activity of silica particles has been reported to also be a function of the ambient conditions such as temperature, pH and nature of the medium.[31]

Despite this wealth of data, the molecular mechanism and the reasons why hemolytic activity differs among different silica samples are still obscure. One reason is that most of the above studies were carried out on a small number of sometimes rather artificial (e.g. spherical Stöber silicas), sometimes poorly characterized, silica samples. A systematic analysis of the surface features responsible for hemolysis by both crystalline and amorphous silicas, adopting a large ensemble of micro and nano-silica forms is therefore needed.

The aim of the present study is to evaluate the hemolytic potential of a large set of silica particles – including a number of "model" silica samples of controlled surface properties and various commercial dusts – to identify the features involved in their hemolytic activity.

The work plan was developed as follows:

- collection of several silica samples in respirable size from various sources, and possibly surface modification through selected treatments (e.g. heating/outgassing at different temperatures, hydrothermal treatment, deposition of aluminium ions);
- particle characterization (e.g. morphology, surface area, size);

- cell-free tests aimed at identifying particulate properties suspected to contribute to the toxic potential (e.g. generation of free radicals, hydrophilicity/hydrophobicity, surface charge), and
- measure of membranolytic activity of the silica samples toward RBCs.

For each property investigated silica samples were grouped into six sets, so that each sample within a group differed as far as possible for only a property, the other features probably implicated in hemolysis being either the same or very similar. Following this approach, difference in the observed hemolytic activity was traced back to a defined property. Physico-chemical properties considered were:

- ability to generate free radicals;
- amorphous or crystalline form;
- morphology, and
- free and H-bonding interacting silanols abundance/distribution.

## MATERIALS AND METHODS

The experimental set considered comprised 15 silica samples of different origin and/or variously modified.

**Silicas.** Pristine silicas (Table 1) were the following:

*Qz–p* was obtained by grinding a very pure quartz crystal from Madagascar in a planetary ball mill (RETSCH S100, GmbH, Haan, Germany) for 3 h (70 rpm), then in the mixer mill (RETSCH MM200) for 9 h (27 Hz). The grinding process was performed in an agate jar to keep silica free from impurities.

Two commercial microcrystalline α-quartz were *Qz(Min-U-Sil 5)* and *Qz(Sigma)*, purchased respectively from U.S. Silica Co. (Berkeley Springs, WV) and Sigma-Aldrich (Milan, Italy).

Vitreous silica (*VS*) was obtained by grinding in a ball mill (agate jar) for 3 h (70 rpm) a very pure silica glass (Suprasil) produced for optical applications.

One amorphous silica (Ångström sphere™) made up of monodispersed silica spheres (*MSS*) was purchased from Fiber Optic Center Inc. (New Bedford, MA).

Aerosil OX 50 (*A50*), a non porous pyrogenic silica obtained by flame hydrolysis of tetrachlorosilane ($SiCl_4$), and *FK320*, a nano-sized precipitated silica, were both from Degussa (Frankfurt A.M., Germany) and kindly supplied by Eigenmann & Veronelli SpA (Milan, Italy). A50 was previously outgassed at 150°C for 2 h.

**Chemical Reagents.** When not otherwise specified, all reagents were purchased from Sigma-Aldrich (Milan, Italy). In all experiments, ultrapure Milli-Q water (Millipore, Billerica, MA) was used.

**Modification of Silicas.**

*Thermal Treatments.* A50, FK320 and Qz(Min-U-Sil 5) were heated in vacuum at 800 or 1000°C for 2 h to reduce the number of silanols, i.e. surface hydrophilicity.[14,23,44] The samples which underwent a thermal treatment are designated by means of a numeral indicating the temperature (°C) of heating, such as with *A50/800°C*.

*Hydrothermal Treatment.* A50 (2.6 g) was suspended in water (75 ml) and heated in a Teflon-lined autoclave at 230°C for 4 h and then dried at room temperature. This treatment leads to an increased abundance of the silanol population.[27] This sample is indicated as *A50/Hydro*.

*Solid State Contamination with Aluminium Ions ($Al^{3+}$).* Qz(Sigma) was ground for 1 h in a ball mill (Retsch, MM2) in corundum ($Al_2O_3$) jars. During the grinding process the quartz particles caused the abrasion of the alumina from the jar and the deposition of aluminium at the quartz surface.[45] The product of this treatment is designated as *Qz(Sigma)/Al*.

**Particle Characterization.**

*Surface area measurements.* The specific surface area of silica samples was assessed by means of the BET method based on $N_2$ adsorption at –196°C, using either an apparatus suitable for quartz (Quantasorb, Quantachrome Instrument) or one suitable for amorphous silica (ASAP 2010, Micromeritics).

*Scanning Electron Microscopy (SEM).* Images were obtained with a Leica Stereo Scan 420 instrument, using a secondary electron detector and with accelerating voltage of 10 kV.

*Particle Size.* Statistical analysis of the particle size distribution was obtained by using a flow particle image analyzer (Sysmex FPIA-3000, Malvern Instruments, U.K., detection range 0.8-300 μm). This instrument measures the diameter of the circle having the same projected area as the particle image detected (i.e. the CE diameter). Measurements were carried out on sample suspensions at a concentration of 1 mg/ml in the same medium (NaCl 0.9%) and keeping the same sonication time as for the hemolysis assay. Each sample was run at least four times with objective lens at 20x magnification in High Power Field (HPF) mode. The four analyses were then pooled to obtain the final size distribution (see Supporting Information, Fig. S1).

*ζ-Potential*. The electrical charge of the particles or their aggregates at pH 7.4 (neutral conditions) and 5.5 (average value for silica suspensions) in water was evaluated by measuring the ζ-potential by means of Electrophoretic Light Scattering (ELS) (Zetasizer Nano-ZS, Malvern Instruments, Worcestershire, U.K.). The silica specimens were suspended (6 mg/10 ml) in ultrapure water and sonicated for 2 min on ice with an ultrasonic probe (100 W, 20 kHz, Sonoplus; Bandelin, Berlin, Germany). The ζ-potential was determined at 25°C after the pH had been adjusted to 7.4 or 5.5 by adding 0.1 M HCl or 0.1 M NaOH.

*Free Radical Detection*. Free radical generation was monitored by means of Electron Paramagnetic Resonance (EPR) spectroscopy (Miniscope 100 EPR spectrometer, Magnettech) and using DMPO (5,5-dimethyl-pirroline-N-oxide) as a trapping agent. EPR

spectra were recorded at room temperature and at a microwave power level of 10 mV, scan range of 120 G, and modulation amplitude of 1 G. All the experiments were repeated at least twice.

*$HO^{\cdot}$ Radical (Fenton Activity).* Each silica sample (75 mg) was suspended in 500 µl of buffered solution (0.5 M potassium phosphate buffer, pH 7.4) and 250 µl of 0.15 M DMPO. The reaction was initiated by adding 500 µl of 0.2 M hydrogen peroxide to the particle suspension, and the radical yield was progressively measured on an aliquot of 50 µl of the suspension for up to 1 h.

*$COO^{\cdot -}$ Radical (Cleavage of a C-H bond).* Each silica sample (75 mg) was suspended in 250 µl of 0.15 M DMPO. The reaction was initiated by adding 250 µl of sodium formate (1.0 M solution in 0.5 M potassium phosphate buffer, pH 7.4) as a target molecule. Carboxyl radical yield was progressively measured on an aliquot of 50 µl of the suspension for up to 1 h.

*Infrared Spectroscopy*. The samples used were compressed to give self supporting pellets suitable for infrared measurement and placed in a quartz cell equipped with KBr windows. Spectra were recorded in the 4000–2500 $cm^{-1}$ region with a FT-IR spectrometer (Bruker Vector 22, equipped with a DTGS detector), using a resolution of 4 $cm^{-1}$ and 128 co-added scans to obtain an acceptable signal-to-noise ratio. The cell used for experiments was attached to a conventional vacuum line (residual pressure $\leq 7.5\times10^{-4}$ Torr) allowing the thermal treatment and adsorption-desorption experiments to be carried out *in situ.*

*Adsorption Microcalorimetry.* Adsorption heat of water vapor was measured at 30°C by means of a heat flow microcalorimeter (Calvet-type, Setaram, France) connected to a high-vacuum gas-volumetric glass apparatus. A well-established stepwise procedure was followed;[46,47] it allows to determine both integral heat evolved and adsorbed amount for small increments of the adsorptive during the same experiment. The equilibrium pressure (p $H_2O$,

Torr) was monitored by means of a transducer gauge (Barocell 0–100 Torr, Edwards). Adsorbed amounts were normalized to the unit surface area ($n_{ads}$, μmol/$m^2$) and plotted in the form of volumetric isotherms. Differential heats of adsorption, which represent the enthalpy changes ($q^{diff} = -\Delta_{ads}H$) associated with the process, were plotted as a function of the increasing water uptake. Prior to the adsorption measurement, samples were outgassed in the calorimetric cells for 2 h at either room temperature or 800°C, and subsequently transferred into the calorimetric vessel without any exposure to the atmosphere.

**Hemolysis Assay of Human RBCs.** Erythrocytes were obtained from fresh human blood of a healthy volunteer donor not receiving any pharmacological treatment. The method used refers to Lu et al., 2009.[15] Blood was collected in a 8.2 ml vacutainer tube containing 0.82 ml of citrate (0.106 mol/l trisodium citrate solution) as anticoagulant. Plasma was separated by centrifugation at 1200g for 10 min (Centrifuge Z364, B. Hermle, Germany). RBCs were then washed four times with NaCl 0.9% (B. Braun Medical, Diegem, Belgium). Following the last wash, the supernatant was removed and the final RBC suspension consisted of 5% by volume in NaCl 0.9%. Each silica type was suspended in NaCl 0.9% immediately before the experiment. The amount of silica was selected to have a surface area of 200 $cm^2$/ml. The suspension was then sonicated during 2 min. The initial suspension was diluted to the final concentrations for experiments (100, 25, 12.5 and 6.25 $cm^2$/ml). Because of the difficulty in dispersing MSS, data in Fig. 3 were obtained by increasing sonication time to 35 min and at the concentration of 100 $cm^2$/ml. Particle suspensions were distributed in quadruplicate in a 96-well plate (150 μl/well) and the RBC suspension was added in all wells (75 μl/well). Negative and positive controls consisted in NaCl 0.9% and Triton-X 100 0.1%, respectively. The plate was incubated at room temperature on an orbital plate shaker for 30 min and then centrifuged at 1200 rpm for 5 min (Sorvall GLC-2B, DuPont Instruments, Newtown, USA). Supernatants were finally transferred to a new plate (75 μl/well) and the absorbance of the

hemoglobin released was determined at a wavelength of 540 nm on a UV/vis spectrophotometer (Infinite 200, Tecan, Grödig, Austria). Absorbance (Abs) values were converted to percentages of hemolysis according to the formula:

$$\%hemolysis = \frac{Abs_{sample} - Abs_{negative\_control}}{Abs_{positive\_control} - Abs_{negative\_control}} * 100$$

To evaluate the role of the surface charge of silica particles in hemolysis,[32] experiments with chloroquine were performed by following the same procedure except that chloroquine (up to 2.6 mM) was added to the mixture of silica (at the constant surface area dose of 100 $cm^2$/ml) and RBCs. In preliminary experiments we verified that, at these doses, chloroquine did not cause hemolysis per se.

**Statistical Analysis.** Hemolytic activity was assessed in at least three independent experiments for all the silica specimens considered. Data are expressed as mean ± standard deviation (SD). The statistical significance of the differences among samples was analyzed using the two-sample Student's t-test when two samples were compared at each dose, or using one-way analysis of variance (ANOVA) with Tukey's post hoc test when more than two samples were compared at each dose. When $p < 0.05$, the difference between groups was considered statistically significant.

## RESULTS

The pristine or modified silica dusts were grouped into 6 sets, each exploring the role of a given physico-chemical property in hemolytic activity. Specimens differed within each set for this one physico-chemical property in order to associate – where possible – differences in the hemolytic effect to differences in this single feature. Table 2 presents the silica samples and the corresponding property/treatment under study. Results in the hemolysis assay are presented according to these six sets. Percentage hemolysis is reported for increasing

concentrations of silica particles, expressed in surface area dose ($cm^2$/ml) (Table 1). The choice of the BET value for surface metric – which comprises all forms of exposed surface including pores, small cracks, interstices with which the cell surface will not be in contact – is debatable. In the present case where a set of particles rather different in nature and often with a heterogeneous distribution of sizes are compared, the BET surface area remains, however, the best reference. Note that porosity is nearly absent and the geometrical/external surface in most cases is impossible to obtain. It is also worth of note that, here, the silica particles were close in size to the facing membrane part with which they interact, so that curvature of both may be determinant in the outcome of the interaction. Hence, a respective adsorbate and adsorbent may probably not be identified in the silica particle/RBC pairs here considered.

All silica particles examined caused a dose-dependent increase in hemolysis, when active. The addition of chloroquine to the mixture of the commercial quartz Qz(Min-U-Sil 5) at the constant concentration of 100 $cm^2$/ml caused a chloroquine dose-dependent decrement in hemolytic activity (see Supporting Information, Fig. S2).

In the following, results relatable to each feature are considered separately.

## Part 1. Hemolytic Activity of Pristine Silicas

**a. Involvement of Free Radicals.** Three kinds of quartz particles, two commercial ones, Qz(Min-U-Sil 5) and Qz(Sigma), and a very pure one Qz-p were considered. The commercial quartz and the pure one differed in abundance and nature of free radical generated, as shown in the inset of Fig. 1 where the EPR spectra of the DMPO adducts with the $^{\cdot}OH$ or $COO^{\cdot -}$ radicals are reported. The two types of commercial quartz (Fig. 1, inset spectra a and b) were able to produce both hydroxyl radicals (from hydrogen peroxide, Fenton activity) and carboxyl radicals (from a homolytic rupture of a C-H bond) to the same extent.[48,49] The pure quartz (Fig. 1, inset spectra c) only exhibited a Fenton-like activity, in agreement with previous findings.[50] All the three samples were hemolytic (Fig. 1) but Qz(Min-U-Sil 5)

showed the highest activity while Qz(Sigma) and Qz-p were not significantly different at any dose investigated, in spite of their differences in free radical release capacity. This is mostly suggestive that free radicals are not involved in hemolysis, in line with several previous reports.[13,19,37] Such inference will be further confirmed by the high hemolytic activity of one pyrogenic silica (see Results, part 1, paragraph d) which did not generate any radical in aqueous suspension, confirming previous results.[51]

**b. Influence of Crystallinity.** Comparison was in this case between the pure quartz Qz-p and a very pure vitreous silica (VS) or "silica glass", a fully amorphous silica obtained by grinding, like quartz dusts. VS features – surface area, size, micromorphology (irregular and jagged edges), hydrophilicity and potential to generate free radicals (Table 1) – were close to those of the pure quartz,[50] opposite to what happens with most other amorphous forms obtained by combustion or precipitation. Crystallinity was thus the only feature discriminating the two samples. Interestingly Qz-p and VS were both hemolytic, VS being even more active than Qz-p (Fig. 2, in the inset the X-rays diffraction patterns), so ruling out the hypothesis that the mere crystallinity might be related to the hemolytic potential of silicas.

**c. Role of Morphology.** Comparison was here carried out between vitreous silica (VS) and a monodispersed amorphous silica (MSS). MSS and VS had similar size (Table 1 and Supporting Information, Fig. S1) but different morphology as reported in the SEM images (inset of Fig. 3). VS consisted of particles with acute edges and spikes; 80% of VS particles ranged from 0.9 to 2.7 μm and had an average CE (Circle Equivalent) diameter of 1.6. MSS was made up of perfectly spherical and smooth particles, with size distribution around 1 μm. Both samples were chemically very pure.[50]

To improve MSS dispersion, the experimental conditions for both silica specimens were in the present case modified (see Materials and Methods). The results for hemolysis are reported

in Fig 3. While VS was hemolytic also in the adapted experimental conditions, MSS was not hemolytic at all. The roundish surface of MSS did not interfere with the RBC membrane.

**d. Preparation Route. Pyrogenic Silica *vs* Precipitated from Aqueous Solutions.** The hemolytic activity of the pyrogenic silica A50 and the precipitated FK320 is reported in Fig. 4B and C (empty bars). A50 was extremely active while FK320 was nearly inert – please note that the related figure (inset in Fig. 4C) has undergone a tenfold magnification. This provides evidence that the preparation procedure markedly determines the surface features related to the hemolytic potential. As both specimens did not generate free radicals,[51] the samples differed in the surface functionalities at the surface, namely silanols -SiOH and siloxane bridges -Si-O-Si-.

To check this hypothesis, surface modifications were carried out to modify the relative abundance of these functionalities in the two amorphous silicas and in the commercial quartz most employed in silica toxicity testing.

**Part 2. Hemolytic Activity of Surface Modified Silicas**

**a. Reduction of the Silanol Population by Heating in Vacuum.** Upon heating, silanols progressively condense into siloxanes with elimination of water[25] (scheme A in Fig. 4).

Two of the amorphous silicas (A50, pyrogenic and FK320, precipitated) and a crystalline one (Min-U-Sil 5) were heated at 800 and 1000°C under vacuum, and then tested for their hemolytic activity (Fig. 4B, C, D). Among pristine samples, the pyrogenic silica A50 (Fig. 4B) was the most active, while the precipitated FK320 (Fig. 4C) was nearly inert. In all three cases, heating up to 800°C resulted in a remarkable loss of the original hemolytic potential, similarly to what previously found with the crystalline silica polymorph cristobalite,[14] whereas no further changes occurred upon heating at 1000°C.

The above data suggested that both the population of polar species and the free/H-bonding interacting silanols play a crucial role in the hemolytic activity of silica. To gain information

on silanol population and on its modification upon heating, the two amorphous silicas A50 and FK320 were submitted to FT-IR investigation. Spectra (Fig. 5) were run in air (a), upon outgassing at room temperature (b), upon heating at 800°C under vacuum (c) and finally upon contact with a substantial water vapor pressure (ca. 20 Torr) (d), which should give an idea of what may happen upon contact with the aqueous solution for hemolysis tests, even if in water aggregation will take place with the smaller particles. All spectra showed a sharp band at 3750 $cm^{-1}$ due to isolated silanols, and broad bands in the range 3750-3000 $cm^{-1}$ related to interacting silanols.[52] The intensity of the broad bands decreased after outgassing at room temperature and, more dramatically, after outgassing at 800°C, due to removal of physisorbed water and to surface dehydroxylation, respectively. The most relevant feature was that water vapor in contact with the samples outgassed at 800°C was taken up only by FK320, the spectrum nearly going back to the pristine situation. It is worth of note that A50 still featured the peak due to isolated silanol species.

To gain information on the rehydration process, water vapor uptake and heat of adsorption were measured on both FK320 and A50 outgassed at room temperature and 800°C (Fig. 6). At both outgassing temperatures the amount of water adsorbed on FK320 was much higher than on A50 (about five fold) (Fig. 6A): the corresponding heat of interaction also indicated a strong interaction of water with FK320 and a relatively weak one on A50 (Fig. 6B). The two silica samples lost a great part of their potential to adsorb water upon heating at 800°C in agreement with previous findings,[44] although the affinity for water in terms of both uptake and energy of interaction remained much larger for FK320.

**b. Increment of Silanols Density by Hydrothermal Treatment.** The reverse process to thermal dehydration is the conversion of siloxanes into silanols by ring opening (reverse reaction of Fig. 4A). A hydrothermal treatment was performed on the A50 sample to increase the population of surface silanols. The hydrothermally-treated sample showed (Fig. 7) an

increased intensity of the broad band in the 3700-3000 $cm^{-1}$ range, in particular the component at ca. 3600 $cm^{-1}$. The hydrothermal treatment thus enhanced silanol density, which implies an increased surface hydrophilicity.[27] The hemolytic potential was increased after hydrothermal treatment for A50 (Fig. 4B), more clearly observed for doses up to 50 $cm^2$/ml, as higher concentrations likely caused saturation. The role of silanols in RBC membranolysis was thus confirmed.

**c. Aluminium at the Surface.** Aluminium at the quartz surface decreases many adverse biological responses related to fibrogenicity.[16,53-58] RBC membranolysis was also reduced on aluminium doped quartz[10,16] and on quartz rich in alumina.[13]

A new mechanochemical procedure was adopted to deposit aluminium ions at silica surface by grinding Qz(Sigma) in a corundum jar. Fig. 8 shows indeed a decrease in the hemolytic potential of Qz(Sigma) after treatment.

## DISCUSSION

The different types of behavior observed with the large panel of silica particles selected to identify the physico-chemical properties involved in RBC membranolysis confirmed, once again, the complexity of the interactions involved. Consistent with what is already known, the main outcome is that more than one single feature govern and modulate the hemolytic activity of silicas, the major actors being size, form of the particle, and population and surface distribution of silanols.

Other factors can be ruled out. Crystallinity is not crucial for inducing hemolysis as the vitreous silica (fully amorphous) was even more hemolytic than the crystalline Qz–p specimen having the same level of purity, particle morphology and particle size distribution.[50] Micromorphology appears somehow related to hemolysis: the roundish surface of MSS was not hemolytic when compared to the indented vitreous silica, similarly to what was found for

cytotoxicity in murine alveolar macrophages.[51] However, similarly roundish particles, but much lower in size, where found hemolytic[33] thus such a morphology is not sufficient to avoid membranolysis. The generation of free radicals may contribute to membrane damage in some cases,[17,18] but not in the present one where free radicals generated by three pure or commercial quartz species did not match with their hemolytic potential, and the most active amorphous silica A50 did not generate any oxygen radical species.

The present data point to a major role played by silanols/siloxanes, as modifications in their ratio and population brought about dramatic variations in the hemolytic potential. Mere hydrophilicity, though, as measured by water uptake or by the overall intensity of the IR bands related to Si-OH stretching, is a too coarse feature to account for the subtle surface functions inducing membranolysis. In fact, the poorly hydrophilic pyrogenic silica A50 increased its hemolytic activity upon increasing silanol density after a hydrothermal treatment (well documented in the IR spectra of Fig. 7); but the density of silanols was definitely larger on the colloidal silica FK320, nearly inert in hemolysis, than on any pristine or treated A50. Therefore, it is not the overall density of silanols that determines the hemolytic activity of silica.

Past and recent literature respectively on crystalline silicas,[13] and on different sets of amorphous NPs, reports that the potential to rupture the RBC membrane does not strictly parallel the damage caused to other cells types (e.g. epithelial, macrophage, etc.) by silica-based materials.

In particular:

i) whereas cytotoxicity increases with decreasing size in nanosilicas, RBC rupture increases with size;[33]

ii) whereas cytotoxicity of mesoporous silica nanorods differing in aspect ratio to macrophage line RAW 264.7 and epithelial A549 cells is not size dependent,

mesoporous silicas with high aspect ratio show lower hemolytic activity than spherical or low aspect ratio ones[40] and,

iii) whereas the aggregation of silica nanoparticles does not affect the cytotoxic activity in macrophages and fibroblasts,[59] it reduces their hemolytic activity.[43]

On the one hand, all these findings introduce the particle curvature as a determinant of hemolysis, and on the other hand, suggest that a direct contact of the silica surface and the cell membrane at specific points of the two surfaces may be responsible for RBC membrane rupture. As already mentioned, no oxygen reactive intermediate originating from the particles tested here and involved in several other toxic manifestations of silica particles (e.g. genotoxicity) may account for hemolysis. If ROS were involved, one could not explain why a decrease in activity is observed when passing from bulk to mesoporous nanosilicas of similar size,[39] and the same potential (related to the overall surface) to produce ROS intermediates.

The strong interaction between silica and the RBC membrane has to be probably sought in a (yet to be defined) concerted surface arrangement of silanols and siloxanes able to match with some epitopes at the RBC membrane. As proposed long time ago by Nash et al. (1966),[60] silanol groups probably act through their hydrogen-donor character by establishing strong hydrogen bonds with some functionalities protruding out of the RBC membrane. The discussion about the precise nature of such silanols (isolated, geminals, terminal of chains) is premature. Significantly, recent literature[8] favors the idea that a 20% fraction of silanols (whatever their nature) are fairly strong acids with a pKa ca. 4, so being able either to transfer protons or exert strong H-bonds. Dissociated silanols may establish electrostatic interactions with the RBC membrane. The role for $-SiO^-$ was confirmed by the reduced hemolytic activity of quartz following deposition of aluminium (Fig. 8) as well as in the presence of the hydrophobic cation chloroquine (see Supporting Information, Fig. S2). Many conflicting theories are reported on the association between surface charge and hemolysis.[10,11,31,38,40,61]

However, in the present case, noticeably there is no correspondence between the mere ζ-potential values at both pH 7.4 and 5.5 and the hemolytic potential of the silica specimens.

Various sites which may interact with silica can be envisaged at the RBC membrane: membrane proteins (secondary amide groups or nitrogen/oxygen in an amide) interacting through H-bonds;[61,62] phosphate ester groups of membrane phospholipids[60], and positive terminals such as quaternary alkylammonium ions (phosphatidylcholines or sphingomyelins) interacting with dissociated silanols.[62] Moreover, on silica surface particularly strained siloxane groups could exhibit polar interactions through the negatively charged oxygen atom, besides dispersion forces. Such interactions may act as H-bond acceptors toward some membrane groups.

As a whole, the present picture confirms the dual role of the undissociated and dissociated silanol groups toward hemolysis as predicted a long time ago.[10] A new feature is, however, added, that is the need for a specific arrangement of several free (dissociated or not) silanols to match with a "hot spot" on the RBC membrane. H-bonding is a directional bond requiring the presence of highly electronegative atoms and a rigid geometry, which explains the high dependence of the hemolytic potential upon the particle curvature. Only under certain circumstances will the silanol groups and siloxanes be in the right position to allow all the interactions – electrostatic and H-bonding – to occur simultaneously on well defined points of the RBC membrane. The form of erythrocytes, so different from other cells, with different curvature from point to point, may in itself account for the unique reaction of RBCs with silicas.

## CONCLUSIONS

The present results obtained with a large number of carefully selected silicas and the thorough study of their physico-chemical features constitute a progress toward the molecular

explanation of the peculiar hemolytic activity of silicas. Hemolysis is the consequence of several physical and chemical interactions. Among these interactions a key role is played by the surface distribution of variously acidic silanols and siloxanes which may give rise to patterns matching with the RBC membrane through mutual H-bonding and electrostatic interactions.

Further developments of the present research may proceed in various ways: interestingly, although hemolysis plays no role in silica-related diseases, the well known silicosis inhibitors aluminium ions[63] and the polymer PVPNO[64] also inhibit hemolysis. Moreover, empiric correlation of hemolysis with pathogenicity has been reported in animal experiments.[65] On the one hand, on the basis of the present findings, a possible correlation between hemolytic activity and cellular reaction involved in the pathogenic responses could be identified. Under these circumstances the use of few physico-chemical features could predict the potential harmful effect of silicas. On the other hand, a computer modeling of the pattern of the most active sites on silica and of the protruding parts of the RBC membrane, associated to the role of the curvature of both surfaces, could allow the precise description of the interactions taking place at the biointerfaces.

AUTHOR INFORMATION

**Corresponding Author**

*Bice Fubini, "G. Scansetti" Interdepartmental Center for Studies on Asbestos and Other Toxic Particulates & Interdepartmental Center for Nanostructured Interfaces and Surfaces, Department of Chemistry, University of Torino, Via P. Giuria 7, 10125 Turin, Italy. Tel: (+39) 0116707566. Fax: (+39) 0116707577. E-mail: bice.fubini@unito.it.

**Funding Sources**

The authors gratefully acknowledge financial support of the Italian Workers' Compensation Authority (INAIL), Piemonte (Italy), to the research, and specifically a doctoral fellowship to CP.

The Zeta-Size Analyzer and the FPIA equipment were acquired by the "G. Scansetti" Interdepartmental Center for Studies on Asbestos and Other Toxic Particulates with a grant from Compagnia di San Paolo.

**Notes**

The authors declare no competing financial interest.

ACKNOWLEDGMENT

Thanks to Dr. G. Magnacca, Department of Chemistry, University of Torino, for help in the IR measurements.

ASSOCIATED CONTENT

**Supporting Information**

Particle size distribution curves obtained by flow particle image analysis; the hemolytic activity of quartz Min-U-Sil 5 with the addition of chloroquine. This material is available free of charge via the Internet at http://pubs.acs.org/.

ABBREVIATIONS

BET, Brunauer, Emmett and Teller; CE, circle equivalent; DMPO, 5,5-dimethyl-pirroline-N-oxide; ELS, electrophoretic light scattering; EPR, electron paramagnetic resonance; FT-IR, Fourier transform infrared; HF, hydrofluoric acid; HPF, high power field; PVPNO, poly(2-vinylpyridine-N-oxide); ROS, reactive oxygen species; SEM, scanning electron microscopy; SSA, specific surface area; TEM, transmission electron microscopy; XRD, X-ray diffraction.

REFERENCES

(1) International Agency for Research on Cancer (IARC) (1987) Silica and some silicates. *IARC Monographs on the Evaluation of Carcinogenic Risks to Humans*, Vol. 42, IARC, Lyon, France.

(2) International Agency for Research on Cancer (IARC) (1997) Silica, some silicates, coal dust and para-aramid fibrils. *IARC Monographs on the Evaluation of Carcinogenic Risks to Humans*, Vol. 68, IARC, Lyon, France.

(3) International Agency for Research on Cancer (IARC) (2012) A review of human carcinogens: arsenic, metals, fibres, and dusts. *IARC Monographs on the Evaluation of Carcinogenic Risks to Humans*, Vol. 100C, IARC, Lyon, France.

(4) Donaldson, K., and Borm, P. J. (1998) The quartz hazard: a variable entity. *Ann. Occup. Hyg. 42*, 287-294.

(5) Donaldson, K., and Seaton, A. (2012) A short history of the toxicology of inhaled particles. *Part. Fibre Toxicol. 9*, 13.

(6) Fubini, B. (1998) Surface chemistry and quartz hazard. *Ann. Occup. Hyg. 42*, 521-530.

(7) Napierska, D., Thomassen, L. C., Lison, D., Martens, J. A., and Hoet, P. H. (2010) The nanosilica hazard: another variable entity. *Part. Fibre Toxicol. 7*, 39.

(8) Rimola, A., Costa, D., Sodupe, M., Lambert, J. F., and Ugliengo, P. (2013) Silica surface features and their role in the adsorption of biomolecules: computational modeling and experiments. *Chem. Rev.* DOI 10.1021/cr3003054.

(9) Harley, J. D., and Margolis, J. (1961) Haemolytic activity of colloidal silica. *Nature 189*, 1010-1011.

(10) Nolan, R. P., Langer, A. M., Harrington, J. S., Oster, G., and Selikoff, I. J. (1981) Quartz hemolysis as related to its surface functionalities. *Environ*. *Res*. *26*, 503-520.

(11) Zhao, Y., Sun, X., Zhang, G., Trewyn, B. G., Slowing, I. I., and Lin, V. S. (2011) Interaction of mesoporous silica nanoparticles with human red blood cell membranes: size and surface effects. *ACS Nano 5*, 1366-1375.

(12) Warheit, D. B., Webb, T. R., Colvin, V. L., Reed, K. L., and Sayes, C. R. (2007) Pulmonary bioassay studies with nanoscale and fine-quartz particles in rats: Toxicity is not dependent upon particle size but on surface characteristics. *Toxicol*. *Sci*. *95*, 270-280.

(13) Clouter, A., Brown, D., Hohr, D., Borm, P., and Donaldson, K. (2001) Inflammatory effects of respirable quartz collected in workplaces versus standard DQ12 quartz: Particle surface correlates. *Toxicol*. *Sci*. *63*, 90-98.

(14) Hemenway, D. R., Absher, M. P., Fubini, B., and Bolis, V. (1993) What is the relationship between hemolytic potential and fibrogenicity of mineral dusts? *Arch*. *Environ*. *Health 48*, 343-347.

(15) Lu, S., Duffin, R., Poland, C., Daly, P., Murphy, F., Drost, E., MacNee, W., Stone, V., and Donaldson, K. (2009) Efficacy of simple short-term in vitro assays for predicting the potential of metal oxide nanoparticles to cause pulmonary inflammation. *Environ*. *Health Perspect*. *117*, 241-247.

(16) Duffin, R., Gilmour, P. S., Schins, R. P. F., Clouter, A., Guy, K., Brown, D. M., MacNee, W., Borm, P. J., Donaldson, K., and Stone, V. (2001) Aluminium lactate treatment

of DQ12 quartz inhibits its ability to cause inflammation, chemokine expression, and nuclear factor-kappa B activation. *Toxicol. Appl. Pharmacol. 176*, 10-17.

(17) Razzaboni, B. L., and Bolsaitis, P. (1990) Evidence of an oxidative mechanism for the hemolytic activity of silica particles. *Environ. Health Perspect. 87*, 337-341.

(18) Zhang, H., Dunphy, D. R., Jiang, X., Meng, H., Sun, B., Tarn, D., Xue, M., Wang, X., Lin, S., Ji, Z., Li, R., Garcia, F. L., Yang, J., Kirk, M. L., Xia, T., Zink, J. I., Nel, A., and Brinker, C. J. (2012) Processing pathway dependence of amorphous silica nanoparticle toxicity: colloidal vs pyrolytic. *J. Am. Chem. Soc. 134*, 15790-15804.

(19) Dalal, N. S., Shi, X. L., and Vallyathan, V. (1990) Role of free radicals in the mechanisms of hemolysis and lipid peroxidation by silica: comparative ESR and cytotoxicity studies. *J. Toxicol. Environ. Health 29*, 307-316.

(20) Vallyathan, V. (1994) Generation of oxygen radicals by minerals and its correlation to cytotoxicity. *Environ. Health Perspect. 102 (Suppl. 10)*, 111-115.

(21) Hemenway, D., Absher, A., Fubini, B., Trombley, L., Vacek, P. M., Volante, M., and Cavenago, A. (1994) Surface functionalities are related to biological response and transport of crystalline silica. *Ann. Occup. Hyg. 38 (Suppl. 1)*, 447-454.

(22) Fubini, B., Zanetti, G., Altilia, S., Tiozzo, R., Lison, D., and Saffiotti, U. (1999) Relationship between surface properties and cellular responses to crystalline silica: studies with heat-treated cristobalite. *Chem. Res. Toxicol. 12*, 737-745.

(23) Fubini, B., Bolis, V., Cavenago, A., and Volante, M. (1995) Physicochemical properties of crystalline silica dusts and their possible implication in various biological responses. *Scand. J. Work Environ. Health 21 (Suppl. 2)*, 9-14.

(24) Fubini, B. (1997) Surface reactivity in the pathogenic response to particulates. *Environ. Health Perspect. 105 (Suppl. 5)*, 1013-1020.

(25) Iler, R. K. (1979) The surface chemistry of silica. In *The chemistry of silica: solubility, polymerization, colloid and surface properties, and biochemistry* pp 622-729, Wiley, New York.

(26) Pandurangi, R. S., Seehra, M. S., Razzaboni, B. L., and Bolsaitis, P. (1990) Surface and bulk infrared modes of crystalline and amorphous silica particles: a study of the relation of surface structure to cytotoxicity of respirable silica. *Environ. Health Perspect. 86*, 327-336.

(27) Fuji, M., Machida, K., Takei, T., Watanabe, T., and Chikazawa, M. (1998) Effect of surface geometric structure on the adhesion force between silica particles. *J. Phys. Chem. B 102*, 8782-8787.

(28) Murashov, V., Harper, M., and Demchuk, E. (2006) Impact of silanol surface density on the toxicity of silica aerosols measured by erythrocyte haemolysis. *J. Occup. Environ. Hyg. 3*, 718-723.

(29) Singh, S. V., Viswanathan, P. N., and Rahman, Q. (1983) Interaction between erythrocyte plasma membrane and silicate dusts. *Environ. Health Perspect. 51*, 55-60.

(30) Hadnagy, W., Marsetz, B., and Idel, H. (2003) Hemolytic activity of crystalline silica – Separated erythrocytes versus whole blood. *Int. J. Hyg. Environ. Health 206*, 103-107.

(31) Shi, J., Hedberg, Y., Lundin, M., Odnevall, W., I, Karlsson, H. L., and Moller, L. (2012) Hemolytic properties of synthetic nano- and porous silica particles: the effect of surface properties and the protection by the plasma corona. *Acta Biomater. 8*, 3478-3490.

(32) Depasse, J. (1978) Interaction between silica and hydrophobic cations. *Br. J. Ind. Med. 35*, 32-34.

(33) Rabolli, V., Thomassen, L. C., Princen, C., Napierska, D., Gonzalez, L., Kirsch-Volders, M., Hoet, P. H., Huaux, F., Kirschhock, C. E., Martens, J. A., and Lison, D. (2010) Influence of size, surface area and microporosity on the in vitro cytotoxic activity of amorphous silica nanoparticles in different cell types. *Nanotoxicology 4*, 307-318.

(34) Depasse, J. (1978) Influence of the sialic acid content of membranes on their sensitivity to silica and aluminate-modified silica. *Environ. Res. 16*, 88-91.

(35) Gun'ko, V. M., Galagan, N. P., Grytsenko, I. V., Zarko, V. I., Oranska, O. I., Osaulenko, V. L., Bogatyrev, V. M., and Turov, V. V. (2007) Interaction of unmodified and partially silylated nanosilica with red blood cells. *Cent. Eur. J. Chem. 5*, 951-969.

(36) Nolan, R. P., Langer, A. M., and Fourcy, A. (1985) Particle size and chemically-induced variability in the membranolytic activity of quartz: preliminary observation. In *In Vitro effects of mineral dusts* (E.G.Beck and J.Bignon, Ed.) pp 39-50, Springer-Verlag, Berlin.

(37) Daniel, L. N., Mao, Y., Wang, T. C., Markey, C. J., Markey, S. P., Shi, X., and Saffiotti, U. (1995) DNA strand breakage, thymine glycol production, and hydroxyl radical generation induced by different samples of crystalline silica in vitro. *Environ. Res. 71*, 60-73.

(38) Slowing, I. I., Wu, C. W., Vivero-Escoto, J. L., and Lin, V. S. Y. (2009) Mesoporous silica nanoparticles for reducing hemolytic activity towards mammalian Red Blood Cells. *Small 5*, 57-62.

(39) Lin, Y. S., and Haynes, C. L. (2010) Impacts of mesoporous silica nanoparticle size, pore ordering, and pore integrity on hemolytic activity. *J. Am. Chem. Soc. 132*, 4834-4842.

(40) Yu, T., Malugin, A., and Ghandehari, H. (2011) Impact of silica nanoparticle design on cellular toxicity and hemolytic activity. *ACS Nano 5*, 5717-5728.

(41) Wiessner, J. H., Mandel, N. S., Sohnle, P. G., and Mandel, G. S. (1989) Effect of particle size on quartz-induced hemolysis and on lung inflammation and fibrosis. *Exp. Lung Res. 15*, 801-812.

(42) Razzaboni, B. L., Bolsaitis, P., Wallace, W. E., and Keane, M. J. (1990) Effect of thermal treatment on the surface characteristics and hemolytic activity of respirable size silica particles. In *Proceedings of the VIIth International Pneumoconiosis Conference* (Baker, E. L., Ed.) pp 215-230, U.S. Department of health and human services, Pittsburgh, PA.

(43) Thomassen, L. C., Rabolli, V., Masschaele, K., Alberto, G., Tomatis, M., Ghiazza, M., Turci, F., Breynaert, E., Martra, G., Kirschhock, C. E., Martens, J. A., Lison, D., and Fubini, B. (2011) Model system to study the influence of aggregation on the hemolytic potential of silica nanoparticles. *Chem. Res. Toxicol. 24*, 1869-1875.

(44) Bolis, V., Fubini, B., Marchese, L., Martra, G., and Costa, D. (1991) Hydrophilic and hydrophobic sites on dehydrated crystalline and amorphous. *J. Chem. Soc., Faraday Trans. 87*, 497-505.

(45) Fenoglio, I., Martra, G., Prandi, L., Tomatis, M., and Fubini, B. (2001) The role of mechanochemistry in the pulmonary toxicity caused by particulate minerals. *J. Mater. Synth. Process. 8*, 145-154.

(46) Fubini, B. (1988) Adsorption calorimetry in surface chemistry. *Thermochim. Acta 135*, 19-29.

(47) Bolis, V., Busco, C., and Ugliengo, P. (2006) Thermodynamic study of water adsorption in high-silica zeolites. *J. Phys. Chem. B 110*, 14849-14859.

(48) Ghiazza, M., Tomatis, M., Doublier, S., Grendene, F., Gazzano, E., Ghigo, D., and Fubini, B. (2013) Carbon in intimate contact with quartz reduces the biological activity of crystalline silica dusts. *Chem. Res. Toxicol. 26*, 46-54.

(49) Ghiazza, M., Scherbart, A. M., Fenoglio, I., Grendene, F., Turci, F., Martra, G., Albrecht, C., Schins, R. P., and Fubini, B. (2011) Surface iron inhibits quartz-induced cytotoxic and inflammatory responses in alveolar macrophages. *Chem. Res. Toxicol. 24*, 99-110.

(50) Ghiazza, M., Polimeni, M., Fenoglio, I., Gazzano, E., Ghigo, D., and Fubini, B. (2010) Does vitreous silica contradict the toxicity of the crystalline silica paradigm? *Chem. Res. Toxicol. 23*, 620-629.

(51) Gazzano, E., Ghiazza, M., Polimeni, M., Bolis, V., Fenoglio, I., Attanasio, A., Mazzucco, G., Fubini, B., and Ghigo, D. (2012) Physicochemical determinants in the cellular responses to nanostructured amorphous silicas. *Toxicol. Sci. 128*, 158-170.

(52) Morrow, B. A., and Gay, I. D. (2000) Infrared and NMR characterization of the silica surface. *Surfactant Sci. Ser.*, 9-34.

(53) Denny, J. J., Robson, W. D., and Irwin, D. A. (1937) The prevention of silicosis by metallic aluminium: first paper. *Can. Med. Assoc. J. 37*, 1-8.

(54) Le Bouffant, L., Daniel, H., and Martin, J. C. (1977) The therapeutic action of aluminium compounds on the development of experimental lesions produced by pure quartz or mixed dust. *Inhaled Part. 4*, 389-400.

(55) Begin, R., Masse, S., Rola-Pleszczynski, M., Martel, M., Desmarais, Y., Geoffroy, M., LeBouffant, L., Daniel, H., and Martin, J. (1986) Aluminum lactate treatment alters the lung biological activity of quartz. *Exp. Lung Res. 10*, 385-399.

(56) Begin, R., Masse, S., Sebastien, P., Martel, M., Bosse, J., Dubois, F., Geoffroy, M., and Labbe, J. (1987) Sustained efficacy of aluminum to reduce quartz toxicity in the lung. *Exp. Lung Res. 13*, 205-222.

(57) Knaapen, A. M., Albrecht, C., Becker, A., Hohr, D., Winzer, A., Haenen, G. R., Borm, P. J. A., and Schins, R. P. F. (2002) DNA damage in lung epithelial cells isolated from rats exposed to quartz: role of surface reactivity and neutrophilic inflammation. *Carcinogenesis 23*, 1111-1120.

(58) Schins, R. P. F., Duffin, R., Hohr, D., Knaapen, A. M., Shi, T. M., Weishaupt, C., Stone, V., Donaldson, K., and Borm, P. J. A. (2002) Surface modification of quartz inhibits toxicity, particle uptake, and oxidative DNA damage in human lung epithelial cells. *Chem. Res. Toxicol. 15*, 1166-1173.

(59) Rabolli, V., Thomassen, L. C., Uwambayinema, F., Martens, J. A., and Lison, D. (2011) The cytotoxic activity of amorphous silica nanoparticles is mainly influenced by surface area and not by aggregation. *Toxicol. Lett. 206*, 197-203.

(60) Nash, T., Allison, A. C., and Harington, J. S. (1966) Physico-chemical properties of silica in relation to its toxicity. *Nature 210*, 259-261.

(61) Summerton, J., and Hoenig, S. (1977) The mechanism of hemolysis by silica and its bearing on silicosis. *Exp. Mol. Pathol. 26*, 113-128.

(62) Iler, R. (1981) The surface chemistry of amorphous synthetic silica: interaction with organic molecules in an aqueous medium. In *Health Effects of Synthetic Silica Particulates* (Dunnom, D., Ed.) pp 3-21, American Society for Testing and Materials, Philadelphia, PA.

(63) Begin, R., Masse, S., Sebastien, P., Martel, M., Geoffroy, M., and Labbe, J. (1987) Late aluminum therapy reduces the cellular activities of simple silicosis in the sheep model. *J. Leukoc. Biol. 41*, 400-406.

(64) Prugger, F., Mallner, B., and Schlipköter, H. W. (1984) Polyvinylpyridine N-oxide (Bay 3504, P-204, PVNO) in the treatment of human silicosis. *Wiener Klin. Wochenschr. 96*, 848-853.

(65) Stalder, K., and Stöber, W. (1965) Haemolytic activity of suspensions of different silica modifications and inert dusts. *Nature 207*, 874-875.

TABLES

**Table 1.** Physicochemical Characteristics of the Pristine Silica Specimens Investigated

| Sample | Origin | Crystallinity[a] | Morphology[b] | SSA[c] ($m^2/g$) | Main metal impurities (% oxides) | Particle size (μm) | | Free radical generation[e] | | ζ-potential (mV) | | Ref. |
|---|---|---|---|---|---|---|---|---|---|---|---|---|
| | | | | | | Average diameter | 90% Value | $HO^{\cdot}$ | $COO^{\cdot -}$ | pH 7.4 | pH 5.5 | |
| Qz-p | ground natural mineral | crystalline | irregular, spikes | 6.1 | absent | $1.4 \pm 0.8$[d] | 2.0[d] | ++ | absent | -61 | -45 | [50] |
| Qz(Min-U-Sil5) | ground natural mineral | crystalline | irregular, spikes | 5.2 | Al 1.4; Fe 0.06 | $1.7 \pm 0.7$[d] | 2.6[d] | ++ | +++ | -69 | -65 | [48] |
| Qz(Sigma) | ground natural mineral | crystalline | irregular, spikes | 7.5 | Al 2.3 | $1.3 \pm 0.7$[d] | 1.9[d] | + | ++ | -63 | -58 | [49] |
| VS | ground fused silica | amorphous | irregular, spikes | 3.1 | absent | $1.6 \pm 1.2$[d] | 2.7[d] | + | absent | -68 | -51 | [50] |
| MSS | Stöber-like silica | amorphous | spherical, smooth | 4.4 | absent | $1.1 \pm 0.5$[d] | 1.5[d] | absent | absent | -71 | -52 | [50] |
| A50 | pyrogenic silica | amorphous | spherical, smooth | 57 | absent | 0.04[b] | | absent | absent | -50 | -35 | [51] |
| FK320 | precipitated silica | amorphous | irregular | 176 | Fe 0.03 | 0.015[b] | | absent | absent | -36 | -31 | [51] |

Legend: + , low; ++ , high; +++ , very high;

[a] Provided by the manufacturer and confirmed by XRD (X-ray Diffraction).

[b] Assessed by SEM (Scanning Electron Microscopy) or TEM (Transmission Electron Microscopy).

[c] Specific Surface Area (SSA) evaluated by BET (Brunauer, Emmett and Teller method).

[d] Evaluated by flow particle image analysis which measure the average diameter expressed as circle equivalent (CE) diameter ± standard deviation. The 90% Value is the value of the CE diameter below which 90 percent of observations fall.

[e] Measured by EPR spectroscopy using the spin trapping technique.

**Table 2.** Summary of the Silica Samples Grouped by Property/Treatment Considered

| Property/Treatment | Sample | Property of interest |
|---|---|---|
| 1. Free radical generation | Qz(Min-U-Sil 5) | $HO^{\cdot}$ and $COO^{\cdot -}$ |
| | Qz(Sigma) | $HO^{\cdot}$ and $COO^{\cdot -}$ |
| | Qz-p | only $HO^{\cdot}$ |
| 2. Crystallinity *vs* amorphous | Qz-p | crystalline |
| | VS | amorphous |
| 3. Micromorphology | MSS | regular, spherical, smooth |
| | VS | irregular, acute spikes, edges |
| 4. Thermal treatment | | |
| Amorphous | A50, A50/800°C, A50/1000°C | different population of silanols: silanol condensation and increase of surface hydrophobicity |
| | FK320, FK320/800°C, FK320/1000°C | |
| Crystalline | Qz(Min-U-Sil 5), Qz(Min-U-Sil 5)/800°C, Qz(Min-U-Sil 5)/1000°C | |
| 5. Hydrothermal treatment | A50, A50/Hydro | increase of silanol population |
| 6. Grinding in corundum jars | Qz(Sigma), Qz(Sigma)/Al | aluminium at the surface |

FIGURE LEGENDS

**Figure 1.** Effect of free radical generation on hemolysis caused by three quartz specimens: Qz(Min-U-Sil 5), Qz(Sigma) and Qz-p. $n$ = 3-5. *$p$ < 0.05, **$p$ < 0.01, and ***$p$ < 0.001 compared with Qz(Min-U-Sil 5) at each dose. Qz(Sigma) and Qz-p are never statistically different from each other at the same dose. In the inset the potential to generate free radicals from aqueous suspensions of Qz(Min-U-Sil 5) (a), Qz(Sigma) (b), and Qz-p (c): (A) $HO^{\cdot}$ radicals generated from $H_2O_2$ via Fenton reaction and (B) $COO^{\cdot -}$ radicals generated following the homolytic cleavage of the C-H bond in sodium formate. Spectra have been recorded after 60 min of incubation.[48,49]

**Figure 2.** Effect of crystallinity on hemolysis caused by a pure quartz (Qz-p) and vitreous silica (VS). $n$ = 3-4. *$p$ < 0.05, and ***$p$ < 0.001 at each dose. In the insets the XRD spectra of Qz-p (A) and VS (B) in the 10-100 2θ range.[50]

**Figure 3.** Implication of micromorphology on hemolysis caused by monodispersed silica spheres (MSS) and vitreous silica (VS). $n$ = 3-4. All values were significantly different ($p$ < 0.001) at each dose. In the inset SEM micrographs of VS (A) and MSS (B).[50]

**Figure 4.** Effect of condensation of silanols into siloxanes with elimination of water following thermal treatments (A) on hemolysis caused by the pyrogenic silica Aerosil 50 (B), the precipitated silica FK320 (C) and the commercial quartz Qz(Min-U-Sil 5) (D). All the three pristine samples were heated at 800 and 1000°C in vacuum. A50 (B) was also treated under hydrothermal conditions (suspended in water, heated in autoclave at 230°C for 4 h and then dried at room temperature) to hydrate the silica surface by siloxanes opening into silanols (reverse reaction of A). In (C) the inset shows a tenfold magnification of the % of hemolysis for FK320. $n$ = 3-6. *$p$ < 0.05, and **$p$ < 0.01 compared with the pristine sample

at each dose. In (D) all values associated to the heated samples were significantly different ($p < 0.001$) from the pristine one.

**Figure 5.** IR spectra of the pyrogenic silica Aerosil 50 (A) and the precipitated one FK320 (B) in the hydroxyl stretching spectral region (4000-2500 $cm^{-1}$). Spectra of both samples were recorded in air (a); after outgassing 2 h at either room temperature (b), or 800°C (c); after outgassing at 800°C and in presence of water vapor pressure (ca. 20 Torr) at room temperature (d).

**Figure 6.** Adsorption of water vapor on the pyrogenic silica Aerosil 50 (round symbols) and the precipitated silica FK320 (square symbols): (A) amount of water adsorbed as a function of the equilibrium pressure; (B) enthalpy of adsorption as a function of water uptake. Samples were outgassed 2 h at either room temperature (full symbols) or 800°C (empty symbols) before water vapor adsorption at T = 30°C.

**Figure 7.** Effect of a hydrothermal treatment on silanol population of the pyrogenic silica Aerosil 50. FT-IR spectra in the hydroxyl stretching spectral region (4000-2500 $cm^{-1}$) of Aerosil 50 before (spectra a and c) and after (spectra b and d) the hydrothermal treatment: (a) and (b) spectra recorded in air, (c) and (d) spectra recorded after outgassing 2 h at room temperature.

**Figure 8.** Effect of aluminium attached via a mechanochemical treatment to the surface of the commercial quartz Qz(Sigma) on hemolysis. $n$ = 3-4. *$p < 0.05$, and **$p < 0.01$ at each dose.

FIGURES

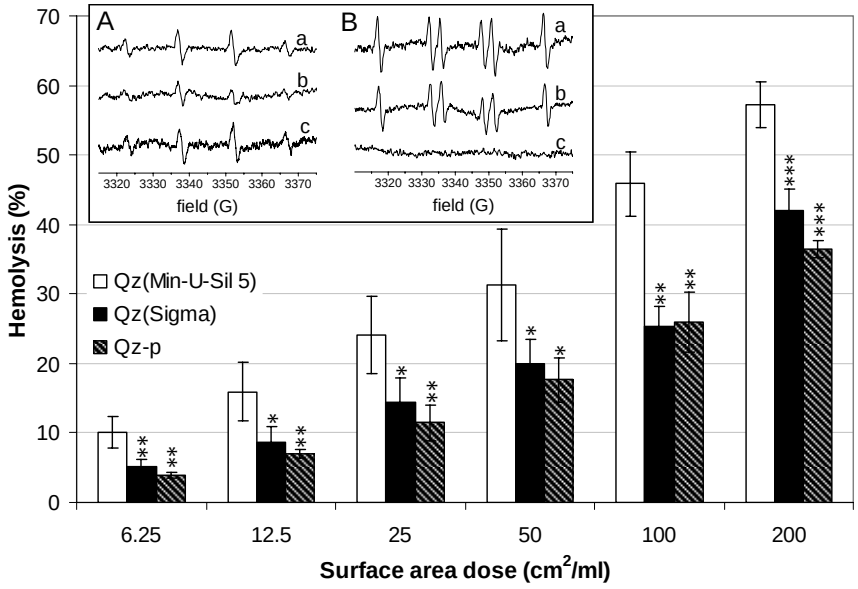


**Figure 1.** Effect of free radical generation on hemolysis caused by three quartz specimens: Qz(Min-U-Sil 5), Qz(Sigma) and Qz-p. $n$ = 3-5. *$p$ < 0.05, **$p$ < 0.01, and ***$p$ < 0.001 compared with Qz(Min-U-Sil 5) at each dose. Qz(Sigma) and Qz-p are never statistically different from each other at the same dose. In the inset the potential to generate free radicals from aqueous suspensions of Qz(Min-U-Sil 5) (a), Qz(Sigma) (b), and Qz-p (c): (A) $HO^{\cdot}$ radicals generated from $H_2O_2$ via Fenton reaction and (B) $COO^{\cdot -}$ radicals generated following the homolytic cleavage of the C-H bond in sodium formate. Spectra have been recorded after 60 min of incubation.[48,49]

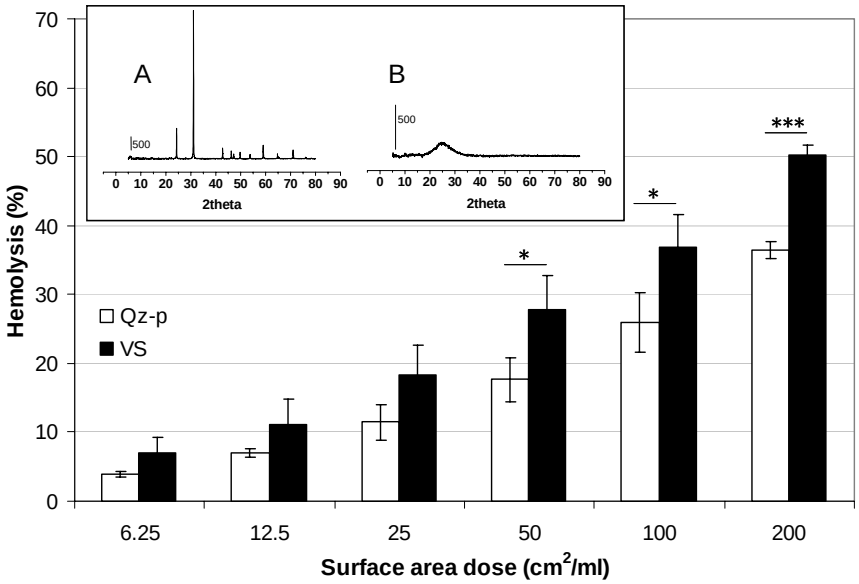


**Figure 2.** Effect of crystallinity on hemolysis caused by a pure quartz (Qz-p) and vitreous silica (VS). $n$ = 3-4. *$p < 0.05$, and ***$p < 0.001$ at each dose. In the insets the XRD spectra of Qz-p (A) and VS (B) in the 10-100 2θ range.[50]

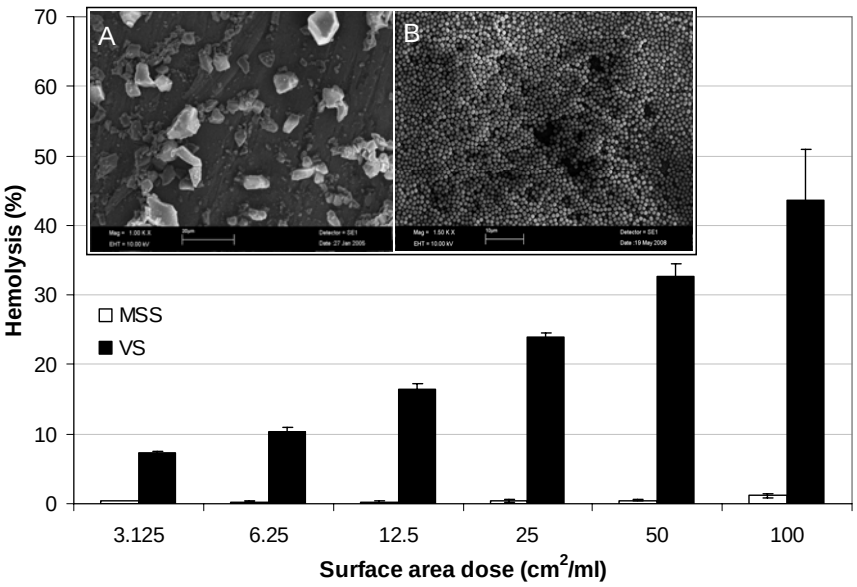


**Figure 3.** Implication of micromorphology on hemolysis caused by monodispersed silica spheres (MSS) and vitreous silica (VS). $n$ = 3-4. All values were significantly different ($p < 0.001$) at each dose. In the inset SEM micrographs of VS (A) and MSS (B).[50]

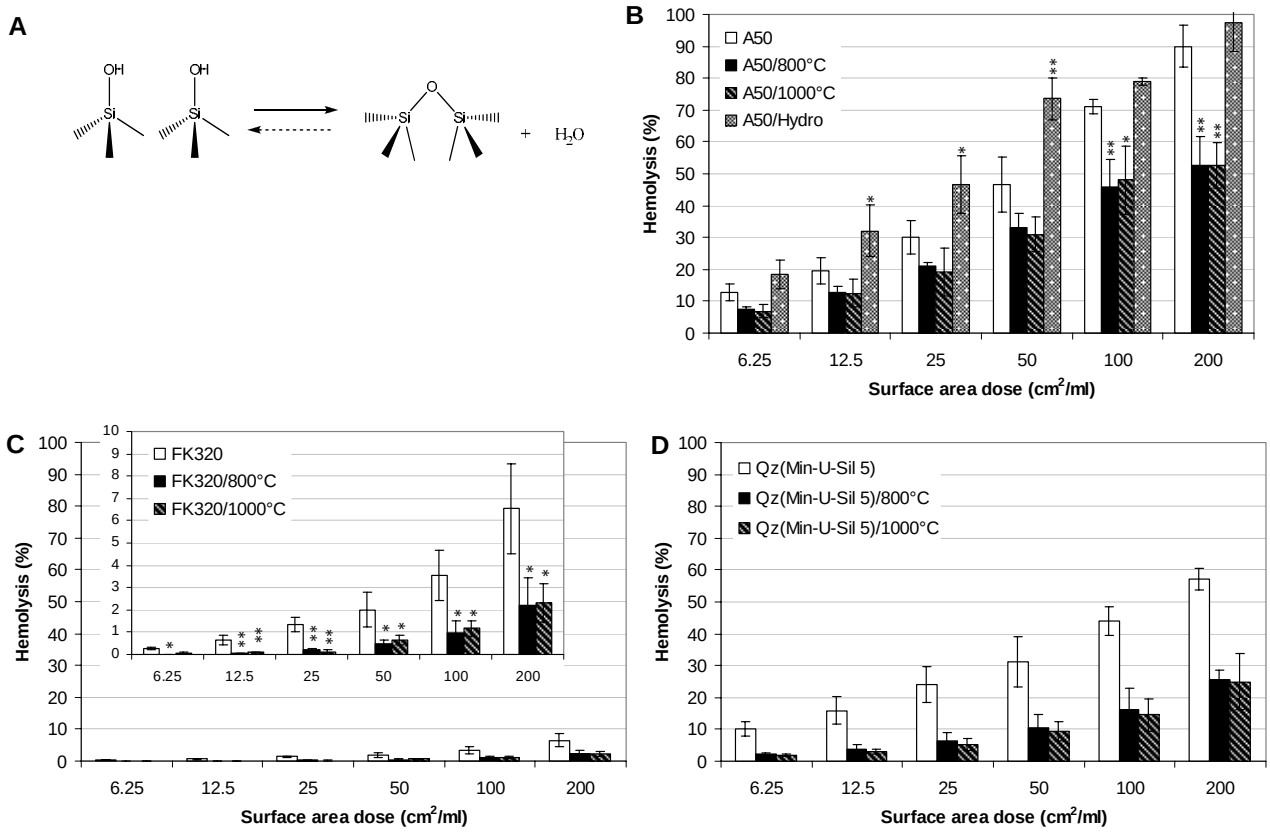


**Figure 4.** Effect of condensation of silanols into siloxanes with elimination of water following thermal treatments (A) on hemolysis caused by the pyrogenic silica Aerosil 50 (B), the precipitated silica FK320 (C) and the commercial quartz Qz(Min-U-Sil 5) (D). All the three pristine samples were heated at 800 and 1000°C in vacuum. A50 (B) was also treated under hydrothermal conditions (suspended in water, heated in autoclave at 230°C for 4 h and then dried at room temperature) to hydrate the silica surface by siloxanes opening into silanols (reverse reaction of A). In (C) the inset shows a tenfold magnification of the % of hemolysis for FK320. $n$ = 3-6. *$p < 0.05$, and **$p < 0.01$ compared with the pristine sample at each dose. In (D) all values associated to the heated samples were significantly different ($p < 0.001$) from the pristine one.

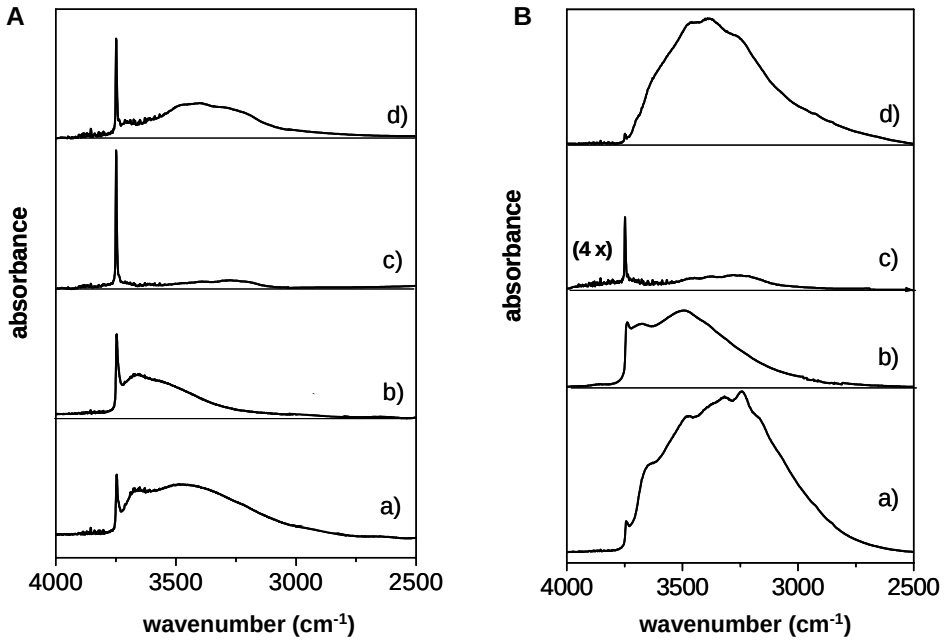


**Figure 5.** IR spectra of the pyrogenic silica Aerosil 50 (A) and the precipitated one FK320 (B) in the hydroxyl stretching spectral region (4000-2500 $cm^{-1}$). Spectra of both samples were recorded in air (a); after outgassing 2 h at either room temperature (b), or 800°C (c); after outgassing at 800°C and in presence of water vapor pressure (ca. 20 Torr) at room temperature (d).

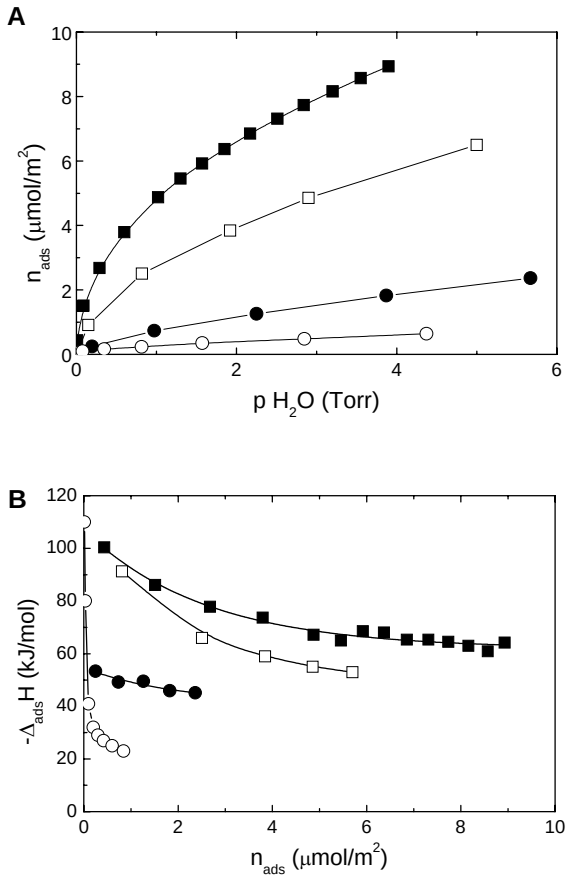


**Figure 6.** Adsorption of water vapor on the pyrogenic silica Aerosil 50 (round symbols) and the precipitated silica FK320 (square symbols): (A) amount of water adsorbed as a function of the equilibrium pressure; (B) enthalpy of adsorption as a function of water uptake. Samples were outgassed 2 h at either room temperature (full symbols) or 800°C (empty symbols) before water vapor adsorption at T = 30°C.

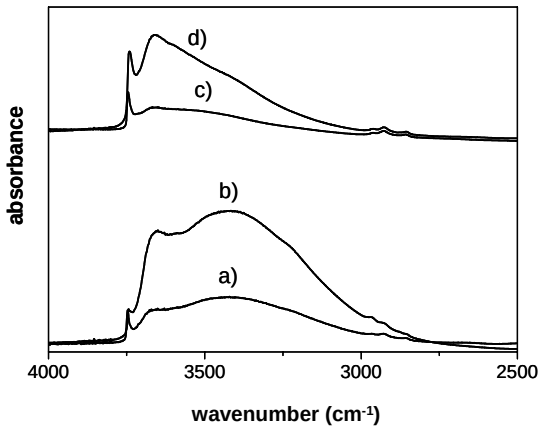


**Figure 7.** Effect of a hydrothermal treatment on silanol population of the pyrogenic silica Aerosil 50. FT-IR spectra in the hydroxyl stretching spectral region (4000-2500 $cm^{-1}$) of Aerosil 50 before (spectra a and c) and after (spectra b and d) the hydrothermal treatment: (a) and (b) spectra recorded in air, (c) and (d) spectra recorded after outgassing 2 h at room temperature.

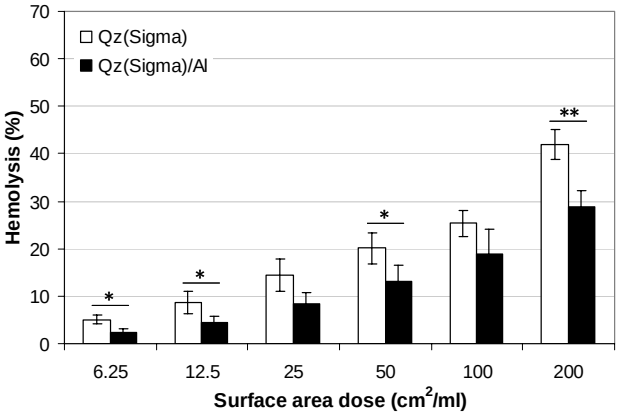


**Figure 8.** Effect of aluminium attached via a mechanochemical treatment to the surface of the commercial quartz Qz(Sigma) on hemolysis. $n$ = 3-4. *$p$ < 0.05, and **$p$ < 0.01 at each dose.